Flexible UWB organic antenna for wearable technologies application

Zahir Hamouda, Jean-Luc Wojkiewicz, Alexander A. Pud, Lamine Kone, Said Bergheul, Tuami Lasri

IET Microwaves, Antennas & Propagation

Research Article

IET Journals
The Institution of Engineering and Technology

Flexible UWB organic antenna for wearable technologies application

ISSN 1751-8725
Received on 11th April 2017
Revised 1st August 2017
Accepted on 18th September 2017
E-First on 8th January 2018
doi: 10.1049/iet-map.2017.0189
www.ietdl.org

Zahir Hamouda[1,2,3], Jean-luc Wojkiewicz[4], Alexander A. Pud[5], Lamine Kone[2], Said Bergheul[1], Tuami Lasri[2] ✉

[1]*Institut d'Aéronautique et des Etudes Spatiales, Université Saad Dahlab, Blida 1, Algeria*
[2]*Institut d'Electronique, de Microélectronique et de Nanotechnologie (IEMN), France*
[3]*Ecole Supérieure des Techniques de l'Aéronautiques (ESTA), Alger, Algeria*
[4]*Mines Douai, SAGE, F-59508 Douai, France*
[5]*Institut of Bioorganic Chemistry and Petrochemistry of NASU, 02160 Kyiv, Ukraine*
✉ *E-mail: tuami.lasri@iemn.univ-lille1.fr*

Abstract: New generations of printed flexible antennas are playing an important role in wireless communication systems. The ultra wide band and wearable possibilities are critical aspects of these kinds of antennas. In this study, the proposed antenna is an elliptical monopole fed by a coplanar waveguide; it uses a kapton substrate and it is optimised to work from 1 to 8 GHz. In the case of copper, a conductive nanocomposite material based on a polymer (polyaniline: PANI) and charged by multiwalled carbon nanotubes (MWCNTs) is exploited. The flexibility of both the kapton substrate and the nanocomposite (PANI/MWCNTs) provides the ability to crumple the antenna paving the way to potential applications for body-worn wireless communications systems. In this study, the performance of the antenna is investigated in terms of return loss, radiation patterns and gain for both crumpled and uncrumpled antennas. The results confirm that performance remains at a good level when the antenna is crumpled.

1 Introduction

In the last decade, ultra wide band (UWB) antennas have received much attention in many different fields. For instance, flexible antennas have been successfully applied to communications service (PCS 1.8/1.9 GHz), wireless local area network (WLAN 2.45 GHz) and wireless networks (around 5.4 GHz) [1–3]. Strategies have been elaborated to develop or adopt a different kind of materials in order to realise flexible printed antennas [4–8].

First, many studies contributed to the performance increase in printed flexible antennas based on copper, silver or gold. Relatively, barely a few research studies were devoted to composite material-based printed flexible antenna. Recently, the demonstration of the benefit in using conductive polymers instead of conventional metals (copper, silver, gold or polyester fibres coated with nickel/zinc-blackened copper) has been made for this type of antennas [9–12].

In particular, conductive polymers such as poly(3,4-ethylenedioxythiophene), polypyrrole (PPy) and polyaniline (PANI) are good contenders for their incorporation in antenna structures, thanks to properties such as flexibility, low cost and the possibility to reshape them [13–17]. Among the different possibilities, PANI has been selected, especially because of its chemical and electrical stability and its very low cost [18]. However, its relatively low conductivity for this application represents a limitation that must be overcome. One of the options retained to increase the conductivity is the addition of carbon nanotubes in the polymer matrix [19–22]. This choice (PANI/MWCNTs) has been made, obviously, on the promise of performance enhancement, thanks to very stable properties (electrical, mechanical and thermal), but also on cost considerations compared to alternative doping solutions based on nano-particles of gold or silver.

The study reported in this paper is dedicated to the development of an UWB flexible printed antenna that can be used for body-worn applications. The crumpling effect on the antenna performance is evaluated through the characterisation of uncrumpled and crumpled versions of the same antenna. The main steps for the fabrication and characterisation of the nanocomposite (PANI/MWCNTs) are outlined in Section 2. The design and fabrication of the nanocomposite-based antenna are described in Section 3. Simulated and measured results of the parameters of interest for crumpled and uncrumpled antennas are presented in Section 4. Finally, some conclusions are drawn in Section 5.

2 PANI/MWCNTs nanocomposite preparation and characterisation

2.1 Materials preparation and film fabrication

Among the conducting polymers available for antenna applications, PANI is very popular, thanks to properties such as facility of synthesis, environmental and chemical stability, controllable electrical conductivity, simplicity in doping, low cost and mechanical flexibility. In this study, the electrically non-conducting emeraldine base (EB) form of PANI-EB was fully protonated with camphor sulphonic acid (CSA) to achieve the conductive polymer form [23]. To improve both polymerisation and conductivity, dichloroacetic acid (DCAA) is used as solvent and secondary dopant at a concentration of 2.85% w/w. This choice reduces the number of π conjugation defects in the polymer backbone [20]. This mixture has demonstrated a very low percolation threshold and a high conductivity [21]. Finally, to improve the mechanical properties of the material, the PANI salt was blended with polyurethane (PU) (Bayer, Desmopan 6065A).

In the following, the preparation of the conductive polymer is briefly described, which consists of two steps. First, PANI-EB and CSA powder are blended with appropriate quantities, in a mortar, to get full protonation of the PANI. Then, this mixture is gradually added into DCAA under strong stirring. To enhance the flexibility feature, a solution including MWCNTs and PU is prepared. After homogenisation and ultrasonication, operations of mixing and stirring are applied to the solutions. Finally, the resulting final solution is then ready to be deposited on a kapton substrate. The adherence of the film to the substrate is found to be very good and validates the fabrication process.

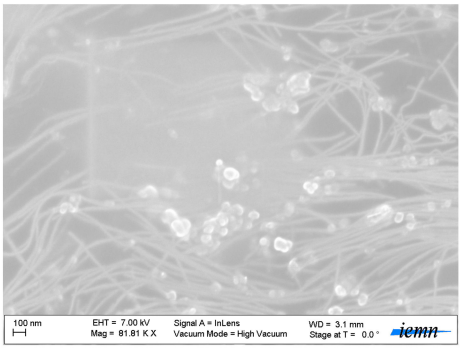

a

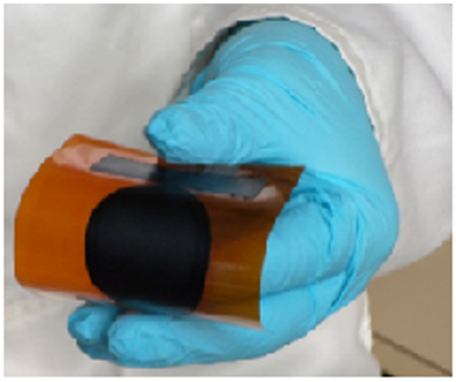

b

Fig. 1 *Formation PANI/MWCNTs nanocomposites*
(a) SEM images of nanocomposite PANI/MWCNTs, ***(b)*** Photograph of the fabricated film

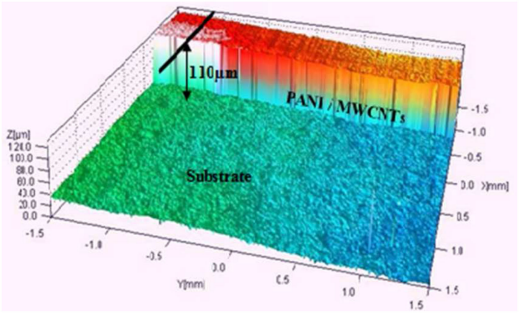

Fig. 2 *Measurement of PANI/MWCNTs film thicknesses by using the Micromeasure TM 2 system*

2.2 SEM morphological analysis

To obtain information about the microstructure of the nanocomposite PANI/MWCNTs, images are gained using scanning electron microscopy (SEM) (Fig. 1*a*).

The different physical properties including roughness, thickness and adhesion of the substrate have been analysed (Fig. 1*b*). Homogeneous distribution of MWCNTs can be seen and a quite uniform coating of MWCNTs with PANI is observed (Fig. 1*a*). The measured diameters of the MWCNTs after PANI layer formation vary from 26 to 29 nm. One can note that the diameter is quite uniform along all the nanotubes. The mean diameter of the MWCNTs used was 20 nm (MWCNTs, supplied by Iljin Nanotech Co., LTD, Seoul). The length of MWCNTs in the nanocomposite is ranged from 10 to 50 µm. The MWCNTs are well embedded and tightly held to the PU matrix, indicating the existence of strong interfacial bonding between the MWCNTs and the PANI. The important bending observed on some of the nanotubes demonstrates good flexibility properties. Finally, some nanotubes assembled in bundles are noticed and some nodules seem to glow.

2.3 Direct current conductivity measurement

The multiwalled carbon nanotubes (MWCNTs) are a very efficient source of electrons. So, the basic idea is to make use of these electrically conductive nano-particles to enhance the conductivity of the polymer. Thus, the PANI and MWCNTs have been added to the PU matrix to form a flexible nanocomposite of high conductivity that enables the fabrication of printed flexible antenna.

In this study, the nanocomposite has been modelled as a thin layer of finite impedance with a sheet resistance R_s estimated through the direct current conductivity σ or the electrical resistivity:

$$R_s = \frac{1}{(h)}$$

where h is the thickness of the film.

The thickness and the surface topography are measured by means of an optical profilometer (Micromeasure TM^2 system, equipped with STIL-DUO). As shown in Fig. 2, the mean thickness of the PANI/MWCNTs film is 110 µm.

The direct current conductivity measured by using the Van Der Pauw method [24] has been found to be 4500 S/m.

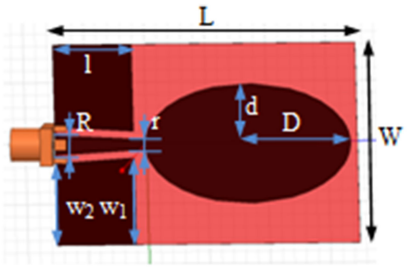

a

b

Fig. 3 *Uncrumpled antenna designed on the kapton substrate*
(a) HSSF® layout view, ***(b)*** Photograph of the realised antenna

3 Design of UWB antennas and fabrication process

The antenna structures were designed and optimised by means of Ansoft's high-frequency structure simulator (HFSS®). It has already been demonstrated that circular- and ellipse-based antennas generally provide better performance compared to conventional microstrip antennas [25, 26]. Our choice is based on the elliptical shape. So, to design the antenna, the coupling between a coplanar waveguide (CPW) and an ellipse patch is exploited (Fig. 3). The material used for both the CPW ground plane and the patch is the nanocomposite PANI/MWCNTs (a thickness of 110 µm). The substrate is a 130 µm-thick kapton (polyimide), in which dielectric properties are $\varepsilon_r = 3.48$ and $\tan(\delta) = 0.002$. The elliptical shape has been retained because it permits, in particular, UWB operation [8, 14, 19, 21, 26–28]. In the case of wearable antennas and because of the various positions taken up by a person, a flexible antenna not only bends but also crumples, especially near the joints. So, to correctly estimate the performance of the antenna, tests under different crumpling conditions are therefore required.

The characteristic impedance of the CPW is designed on the basis of a 50 Ω matching. The geometry of the antenna structure is depicted in Fig. 3. The optimised dimensions are reported in Table 1 (T is the substrate thickness).

Table 1 Parameters of PANI/MWCNTs UWB organic flexible printed antenna

Dimension of substrate, mm						
L		*W*			*T*	
48		34.9			0.13	
patch material = PANI/MWCNTs						
thickness = 0.11 mm						
Dimension of the uncrumpled antenna, mm						
D	*d*	*R*	*r*	W_1	W_2	*l*
16	8.8	3.5	2.5	15	14.5	13

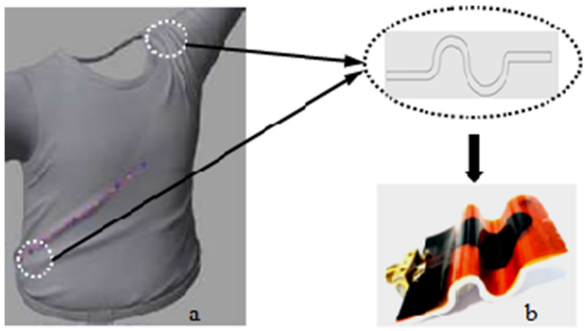

Fig. 4 *Effect of the bending of clothes on the antenna shape*
(a) Bending of the clothes in multiple directions [29], ***(b)*** The photograph of the realised crumpled antenna

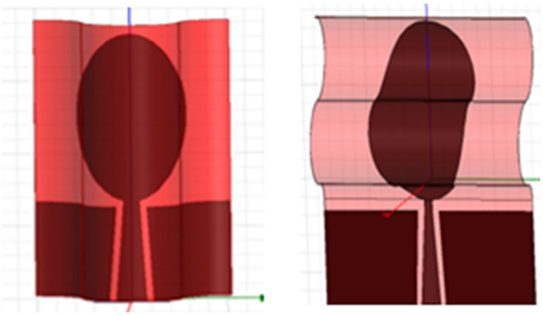

Fig. 5 *HFSS® layout view of crumpled antenna in the x- and y-directions*

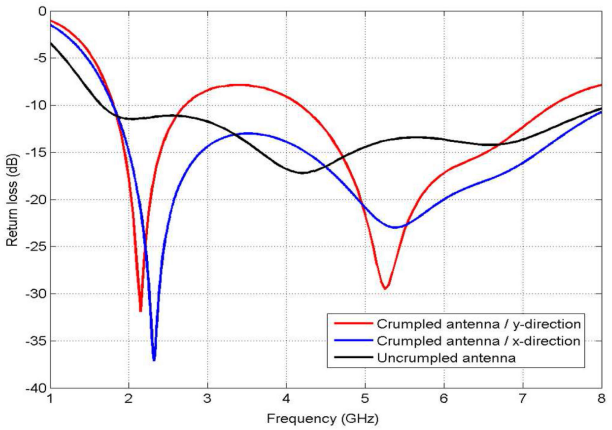

Fig. 6 *Simulation of the return losses for a bending in the x- and y-directions*

An antenna put onto clothes changes its shape with human body movements which results in a variation of its characteristics (radiation pattern, reflection coefficient etc.). The antenna proposed has the ability to follow these movements and to keep its main characteristics. The influence of the crumpling on the antenna performance has been studied by bending the uncrumpled antenna with different angles as illustrated in Fig. 4.

Thanks to 3D printing, the fabrication of antenna supports to mimic crumpled antenna shapes is now easier. Different supports in acrylonitrile butadiene styrene have been realised using Solid work® software.

4 Simulation and measurement results

A complete simulation study has been achieved and the characteristics of the antenna have been investigated in both directions, *x* and *y* (Fig. 5).

In the following, we show the simulations for both directions in terms of return loss (Fig. 6) and radiation patterns (Fig. 7).

The simulated antenna reflection coefficients are shown in Fig. 6 for the three cases of interest, bending along the *x*-axis, bending along the *y*-axis and no crumpling. For both bending directions, a good impedance matching (return loss below −10 dB), especially at WLAN and wireless networks frequency bands, is maintained. In the case of *y*-axis bending, a pretty large bandwidth from 5 to 6 GHz is obtained and a significant resonance with a return loss around −30 dB is attained at 5.2 GHz. Additionally, the response is relatively well balanced with a return loss also around −30 dB at 2.2 GHz which makes this pattern slightly different from the patterns obtained for the *x*-axis bending and uncrumpled antenna.

By concerning the radiation patterns, one can see that the shapes are practically the same in the E-plane for both directions. In the H-plane, the difference between the results obtained for the two directions is more pronounced, particularly for higher frequencies (5.4 and 5.8 GHz).

This preliminary simulation study allows us to conclude that the results obtained for the proposed PANI /MWCNTs antenna, bended in *x*- or *y*-direction, are good enough to be used in many applications (body-worn application). However, once again, as in the real world the situation that is essentially encountered is more likely a bending in the *y*-direction we have realised the antenna in this configuration. In addition, the different simulation tests have shown that the bending in the *y*-direction has the strongest effect on the antenna gain.

In fact, to study the bending impact more finely on the antenna settings, we have examined both positive and negative bendings in the *y*-direction. According to the transmission line model, the elliptical monopole element can be treated as a line resonator with no transverse field variations. The radiator may be represented as two radiating slots along the feeding direction. In the case of the crumpled antenna with positive bending, the radiation of two radiating slots is in the same direction (Fig. 8*a*), so the radiation in the far field is improved (superposition). When the bending is on the other side (negative bending), the effect is much less pronounced. Therefore, the gain value of the crumpled antenna is not improved as much in this situation. As the radiation of the two radiating slots is not in the same direction (Fig. 8*b*), the radiation in the far field is therefore degraded compared to the previous bending.

To verify this conclusion, a simulation study has been done using HFSS®. The current flow observed in three cases – uncrumpled antenna and crumpled antenna bended in positive and negative sides – is shown in Fig. 9.

One can observe that as for the negative bending, the current flow in the uncrumpled case is more perturbed compared to the positive bending leading to a lower gain.

Fig. 10 presents the influence of changing the radius ratio of the ellipse on the performance of the crumpled antenna. The simulation results for the uncrumpled antenna are also added to the

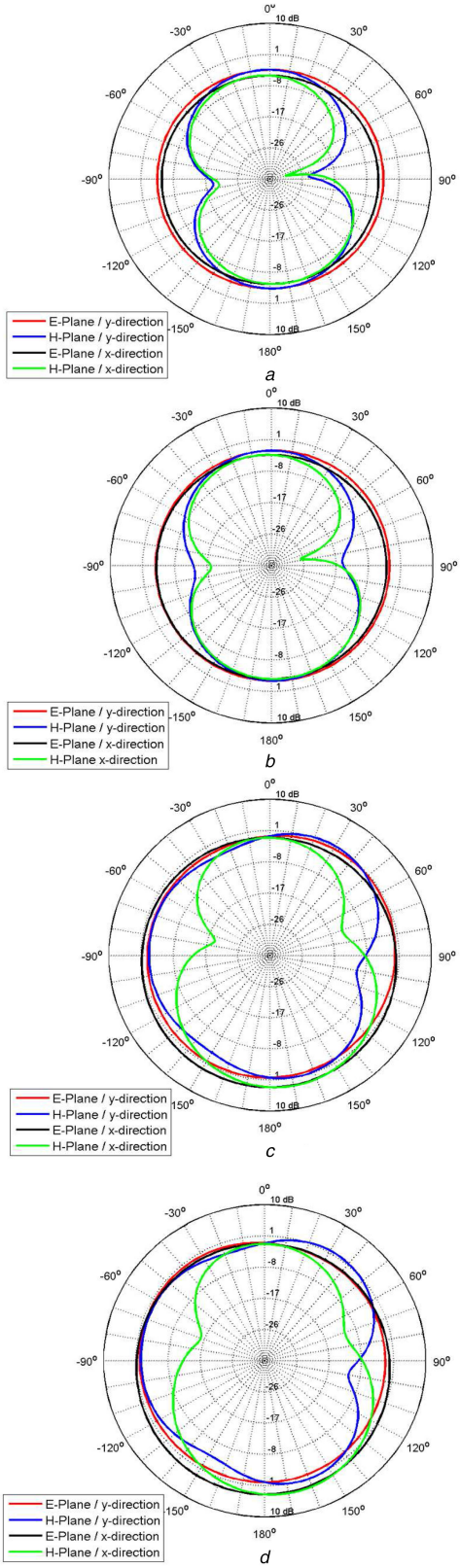

Fig. 7 *Simulated radiation patterns for both the x- and y-directions*

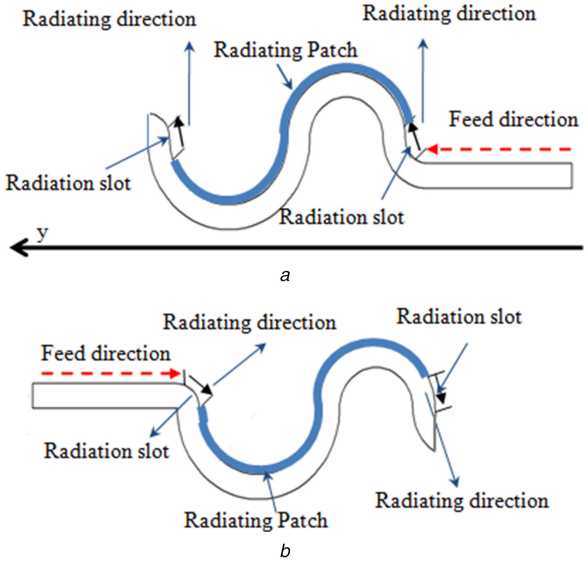

Fig. 8 *Schematic of the antenna radiation*
(a) Positive bending, ***(b)*** Negative bending

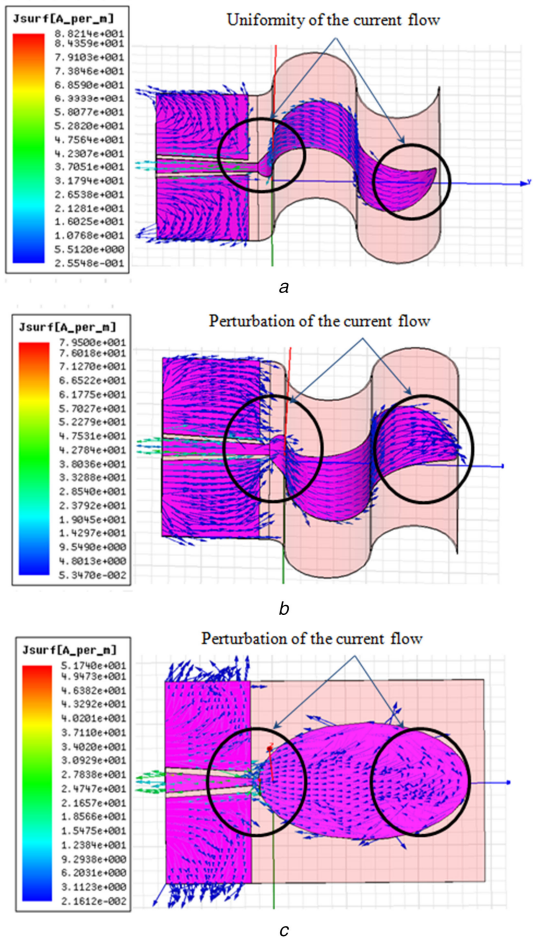

Fig. 9 *Schematic of the current flow at 2.45 GHz (crumpled antenna and uncrumpled antenna)*
(a) Positive bending, ***(b)*** Negative bending, ***(c)*** Uncrumpled antenna

figure for comparison purposes. The bending of the antenna leads to the appearance of two reflection resonance peaks situated around 2.2 and 5.3 GHz. One can also notice that the ratio that gives the best results is 0.55 (D/d; Fig. 3*a*). The radius of curvature, optimised to obtain the best antenna performance at the frequencies of interest, has been found to be 5.3 mm. This data is used to fabricate the antenna by using a 3D-printed support which permits a good control of the antenna shape and dimensions.

Based on the simulation study, two flexible organic antennas have been fabricated (Figs. 3*b* and 4*b*). The return loss properties were measured with an Agilent PNA-X series N5242A network analyser (10 MHz–26.5 GHz). Fig. 11 gives the simulated and measured return loss spectra of uncrumpled and crumpled antennas ($D/d = 0.55$).

First, we notice that crumpled and uncrumpled antennas present an ultra-large frequency bandwidth. However, a non-operation bandwidth of 2.7–4 GHz appeared in the case of the crumpled antenna. We also note that the matching is improved at the resonant frequency. Moreover, a relatively good agreement between the

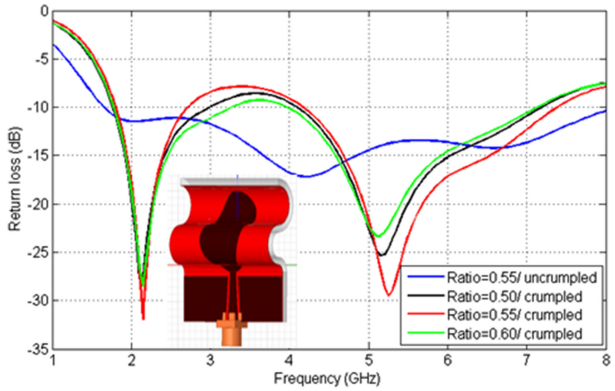

Fig. 10 *Simulation of the crumpling and the ellipse radius ratio effect on antenna return loss (radius of curvature = 5.3 mm)*

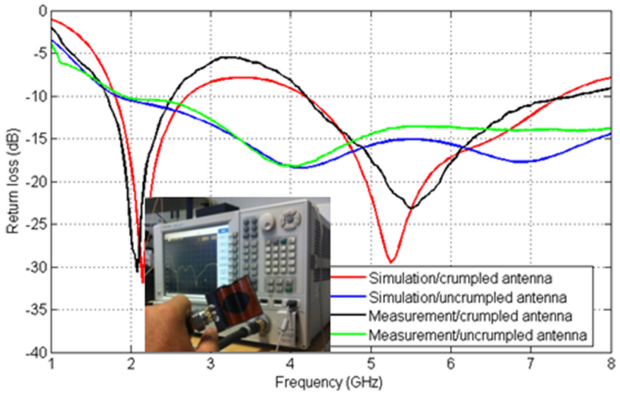

Fig. 11 *Return loss characteristics of the uncrumpled and crumpled antennas*

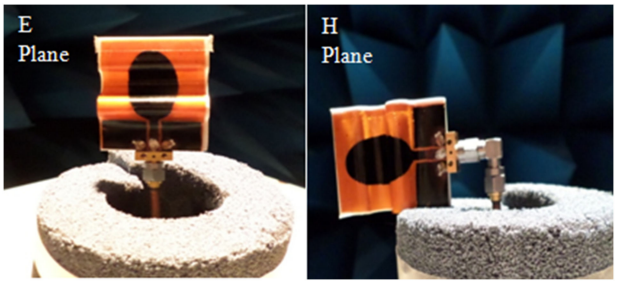

Fig. 12 *Measurement of the radiation patterns and gain of the realised PANI/MWCNTs antenna*

simulation and measurement results is observed. For the crumpled antenna, a return loss of −32 dB at 2.2 GHz with a −10 dB bandwidth of 45% is obtained in the simulation study when the measured return loss is −30 dB at 2.1 GHz with a −10 dB bandwidth of 43%. For the second band, the simulated return loss is −29 dB at 5.3 GHz with a −10 dB bandwidth of 60% while the measured return loss is −23 dB at 5.5 GHz with a −10 dB bandwidth of 62%. All these results together demonstrate that the composite-based antenna proposed (PANI/MWCNTs) presents comparable performance in terms of bandwidth to conventional antennas.

The radiation pattern of an antenna is one of its most fundamental properties. Therefore, it is necessary to measure the radiation patterns of the proposed antennas (uncrumpled and crumpled). This characterisation part has been achieved in the IEMN anechoic chamber by measuring the co-polarisation and the cross-polarisation radiation patterns (planes E and H). The measurement set-up for radiation patterns and gains measurements is shown in Fig. 12. All measurements were obtained by using an Agilent 8735ES vector network analyser (30 kHz–6 GHz) and a standard horn antenna (SAS–200/571). The frequencies selected for the two cases (uncrumpled and crumpled) are 1.9, 2.45, 5.4 and 5.8 GHz.

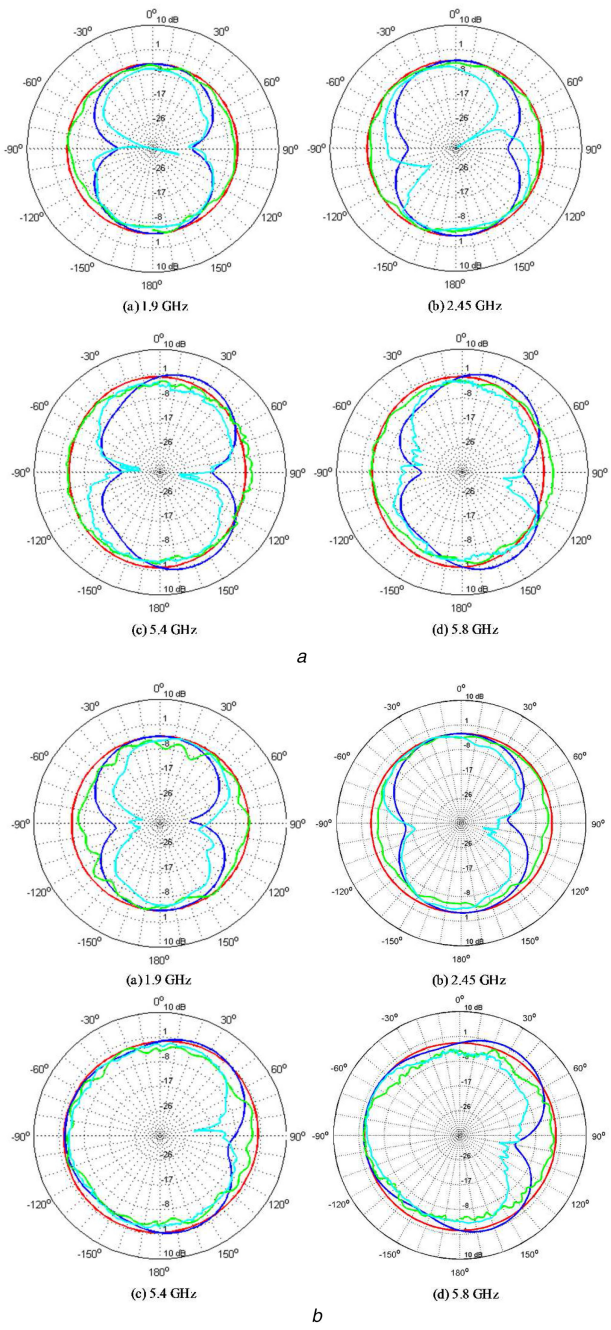

Fig. 13 *Simulated and measured E- and H-planes of far-field radiation patterns (co-polar) of the antenna at each frequency band. Red: E-plane simulation, green: E-plane measurement, blue: H-plane simulation, cyan: H-plane measurement*

(a) Uncrumpled antenna, ***(b)*** Crumpled antenna

The measured co-polarisation radiation patterns for the uncrumpled (Fig. 3*b*) and crumpled (Fig. 4*b*) antennas in the E- and H-planes are compared to the simulated ones in Figs. 13*a* and *b*. Where we can observe a radiation pattern which behaves well, it is seen that the E-plane patterns are omnidirectional, while the H-plane patterns are bidirectional. It is also noticed that the crumpled antenna offers a stable radiation performance over the frequency range of interest.

In the case of the crumpled antenna, we have also measured the cross-polarisation radiation patterns in the E- and H-planes and compared them with the simulated ones (Fig. 14).

The apparition of small ripples on the measured data is mainly caused by the vibration of the proposed antenna while conducting the measurement and by the distribution of the MWCNTs in the nanocomposite matrix (PANI/PU). The cross-polarisation patterns for crumpled antenna show a dipole characteristic, with the minimum gain in the E-plane at 0° and 180°, and the maximum

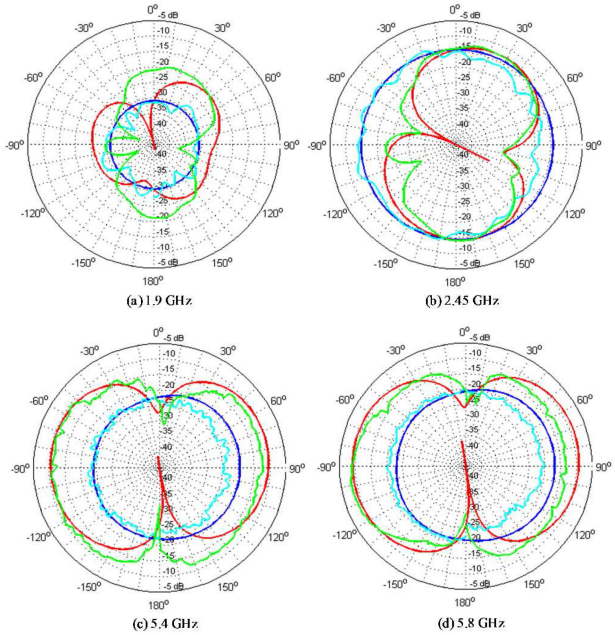

Fig. 14 *Simulated and measured E- and H-planes of far-field radiation patterns (cross-polar) of the crumpled antenna at each frequency band. Red: E-plane simulation, green: E-plane measurement, blue: H-plane simulation, cyan: H-plane measurement*

Table 2 Antenna maximum gain across the selected frequency

Frequency, GHz	Simulated, dBi	Measured, dBi
	Uncrumpled antenna gain	
1.9	−1.85	−2.12
2.45	−1.20	−1.52
5.4	1.45	1.05
5.8	2.21	1.86
	Crumpled antenna gain	
1.9	−1.25	−1.62
2.45	0.13	−0.08
5.4	2.96	2.53
5.8	3.31	3.10

Table 3 Characteristics of the proposed antenna compared to antennas available in the literature

N	Antenna	Antenna conductive material	Bandwidth, GHz	Max gain	Type of antenna
1	[23]	copper	2.2–12.8	4 dBi	non-organic
2	[24]	copper	2–12	4 dBi	non-organic
3	[26]	sliver nano-particles	2–14	4.8 dBi at 5 GHz	non-organic
4	[12]	polyester fibers coated with nickel/zinc-blackened copper	1–25	3 dBi at 5 GHz	non-organic
5	[15]	conductive polymer (PEDOT)	1–20	1.1 dBi at 3 GHz	organic
6	[16]	conductive polymer (PEDOT and PPy)	3.1–10.6	>1 dBi	organic
7	proposed antenna	conductive polymer (PANI/MWCNTs)	1–8	3.1 dBi at 5.8 GHz	organic

gain at ± 90°. The value of cross-polarisation is low, always <−10 dB, which shows the good performance of the antenna. Also, a relatively good agreement between simulations and measurement is noticed. However, higher cross-polarisation components were obtained for measurements, probably due to the impact of the fabrication inconsistencies and the effect of the SMA connector.

Another important parameter that describes the performance of an antenna is the gain. The comparison between the simulated and the measured gains of the proposed antennas is given in Table 2.

The agreement between measured and simulated results for both uncrumpled and crumpled antennas is quite good. One can notice that a slightly higher gain is obtained for the crumpled antenna. This observation was already made in the case of the simulation study where it was shown that the current flow is less perturbed in the case of the crumpled antenna, resulting in a higher gain compared to the uncrumpled antenna. Finally, it can be noticed that the maximum measured gain is higher than 3 dBi at 5.8 GHz.

All these results demonstrate that this antenna is a good candidate for the applications targeted. In Table 3, we compare the solution proposed to other possibilities found in the literature.

From this table, it can be seen that among the organic solutions, the antenna proposed demonstrates the higher gain with a quite large bandwidth, leastwise sufficient for the application aimed.

5 Conclusion

Conductive polymers have drawn significant attention in the microwave community, thanks to their potential application in many fields. They are particularly attractive in fabricating antennas. In this paper, the influence of bending on the characteristics of a flexible conductive polymer-based UWB organic printed antenna is investigated. The composite polymer fabricated is PANI charged by MWCNTs. A good agreement between the experimental and simulation results has proven the suitability of the solution proposed in situations where the antenna

could be crumpled. Actually, the small discrepancies observed are mainly attributed to some parameters variation during the fabrication process and measurement conditions. The maximum gain measured at 5.8 GHz is, respectively, of 1.86 and 3.1 dBi for uncrumpled and crumpled antennas. Moreover, the gain of the organic flexible antenna (PANI/MWCNTs) proposed could be adjusted by modifying the conductivity of the polymer through the variation of MWNCTs concentration in the PANI matrix. The performance of this organic UWB monopole antenna is outstanding compared to what has already been published in the literature for comparable organic antennas. One of the future applications of this antenna is in the field of wireless communications. In particular, the crumpling property allows integrating this kind of antennas onto clothes without impairing a lot its mechanical and electrical properties.

6 References

[1] Haiwen, L., Shuangshuang, Z., Pin, W., *et al.*: 'Flexible CPW-fed fishtail-shaped antenna for dual-band applications', *IEEE Antennas Wirel. Propag. Lett.*, 2014, **13**, pp. 770–773

[2] Bai, Q., Langley, R.: 'Crumpling of PIFA textile antenna', *IEEE Trans. Antennas Propag.*, 2012, **60**, (1), pp. 63–70

[3] Liu, L., Zhu, S., Langley, R.: 'Dual-band triangular patch antenna with modified ground plane', *Electron. Lett.*, 2007, **43**, (3), pp. 140–141

[4] Nikolaou, S., Ponchak, G.E., Papapolymerou, J., *et al.*: 'Conformal double exponentially tapered slot antenna (DETSA) on LCP for UWB applications', *IEEE Trans. Antennas Propag.*, 2006, **54**, (6), pp. 1663–1669

[5] DeJean, G., Bairavasubramanian, R., Thompson, D., *et al.*: 'Liquid crystal polymer (LCP): a new organic material for the development of multilayer dual-frequency/dual-polarization flexible antenna arrays', *IEEE Antennas Wirel. Propag. Lett.*, 2005, **4**, (1), pp. 22–26

[6] Lin, C.P., Chang, C.H., Cheng, Y.T., *et al.*: 'Development of a flexible SU-8/PDMS-based antenna', *IEEE Antennas Wirel. Propag. Lett.*, 2011, **10**, pp. 1108–1111

[7] Wang, Z., Zhang, L., Bayram, Y., *et al.*: 'Embroidered conductive fibers on polymer composite for conformal antennas', *IEEE Trans. Antennas Propag.*, 2012, **60**, (9), pp. 4141–4147

[8] Khaleel, H.R., Al-Rizzo, H.M., Rucker, D.G.: 'Compact polyimide-based antennas for flexible displays', *J. Disp. Technol.*, 2012, **8**, (2), pp. 91–97

[9] Kiourti, A., Volakis, J.L.: 'Stretchable and flexible E-fiber wire antennas embedded in polymer', *IEEE Antennas Wirel. Propag. Lett.*, 2014, **13**, pp. 1381–1384

[10] Janeczek, K., Jakubowska, M., Kozioł, G., *et al.*: 'Investigation of ultra-high-frequency antennas printed with polymer pastes on flexible substrates', *IET Microw. Antennas Propag.*, 2012, **6**, (5), pp. 549–555

[11] Mebdipour, A., Rosca, I.D., Sebak, A.R., *et al.*: 'Carbon nanotube composites for wideband milimetrer-wave antenna application', *IEEE Trans. Antenna Propag.*, 2011, **59**, pp. 3572–3578

[12] Elobaid, H.A.E., Rahim, S.K.A., Himdi, M., *et al.*: 'A transparent and flexible polymer-fabric tissue UWB antenna for future wireless networks', *IEEE Antennas Wirel. Propag. Lett.*, 2017, **16**, pp. 1333–1336

[13] Fenelon, A.M., Breslin, C.B.: 'The electrochemical synthesis of polypyrrole at a copper electrode: corrosion protection properties', *Electrochim. Acta*, 2002, **47**, (28), pp. 4467–4476

[14] Iroh, J.O., Zhu, Y., Shah, K., *et al.*: 'Electrochemical synthesis: a novel technique for processing multi-functional coatings', *Prog. Org. Coat.*, 2003, **47**, (3), pp. 365–375

[15] Kaufmann, T., Verma, A., Truong, V.T., *et al.*: 'Efficiency of a compact elliptical planar ultra-wideband antenna based on conductive polymers', *Int. J. Antennas Propag.*, 2012, pp. 1–11

[16] Chen, S.J., Kaufmann, T., Shepherd, R., *et al.*: 'A compact, highly efficient and flexible polymer ultra-wideband antenna', *IEEE Antennas Wirel. Propag. Lett.*, 2015, **14**, pp. 1207–1210

[17] Chen, S.J., Fumeaux, C., Talemi, P., *et al.*: 'Progress in conductive polymer antennas based on free-standing polypyrrole and PEDOT: PSS'. IEEE, 17th Int. Symp. Antenna Technology and Applied Electromagnetics (ANTEM), Montreal, Canada, July 2016, pp. 1–4

[18] Oueiny, C., Berlioz, S., Perrin, F.X.: 'Carbon nanotube–polyaniline composites', *Prog. Polym. Sci.*, 2014, **39**, (4), pp. 707–748

[19] Hamouda, Z., Wojkiewicz, J.L., Pud, A.A., *et al.*: 'CPW-fed dual band monopole antenna based on conductive polymers'. 9th European Conf. Antennas and Propagation (EuCAP 2015), Portugal, Lisbon, May 2015, pp. 1–4

[20] Hamouda, Z., Wojkiewicz, J.L., Pud, A.A., *et al.*: 'Design fabrication and characterisation of polyaniline and multiwall carbon nanotubes composites-based patch antenna', *IET Microw. Antennas Propag.*, 2016, **10**, (1), pp. 88–93

[21] Hamouda, Z., Wojkiewicz, J.L., Pud, A.A., *et al.*: 'Dual band elliptical planar conductive polymer antenna printed on a flexible substrate', *IEEE Trans. Antennas Propag.*, 2015, **63**, (12), pp. 5864–5867

[22] Hamouda, Z., Wojkiewicz, J.L., Pud, A.A., *et al.*: 'Development of a patch antenna based on a polyaniline/carbon coated cobalt composite'. 10th European Conf. Antennas and Propagation (EuCAP 2016), Davos, Switzerland, April 2016, pp. 1–4

[23] Cao, Y., Smith, P., Heeger, A.J.: 'Counter-ion induced processibility of conducting polyaniline', *Synth. Met.*, 1993, **57**, (1), pp. 3514–3519

[24] Hoang, N.H., Wojkiewicz, J.L., Miane, J.L., *et al.*: 'Lightweight electromagnetic shields using optimized polyaniline composites in the microwave band', *Polym. Adv. Technol.*, 2007, **18**, (4), pp. 257–262

[25] Sarkar, D., Srivastava, K.V., Saurav, K.: 'A compact microstrip-fed triple band-notched UWB monopole antenna', *IEEE Antennas Wirel. Propag. Lett.*, 2014, **13**, pp. 396–399

[26] Sun, Y., Cheung, S.W., Yuk, T.I.: 'Design of a textile ultra-wideband antenna with stable performance for body-centric wireless communications', *IET Microw. Antennas Propag.*, 2014, **8**, (15), pp. 1363–1375

[27] Khaleel, H.R., Al Rizzo, H.M., Rucker, D.G., *et al.*: 'A compact polyimide-based UWB antenna for flexible electronics', *IEEE Antennas Wirel. Propag. Lett.*, 2012, **11**, pp. 564–567

[28] Wang, C.J., Hsiao, K.L.: 'CPW-fed monopole antenna for multiple system integration', *IEEE Trans. Antennas Propag.*, 2014, **62**, (2), pp. 1007–1011

[29] Cutler, L.D., Gershbein, R., Wang, X.C., *et al.*: 'An art-directed wrinkle system for CG character clothing'. Proc. ACM SIGGRAPH/Eurographics Symp. Computer Animation, July 2005, pp. 117–125